World's first spaceflight on-orbit demonstration of a flexible solar array system based on shape memory polymer composites

LAN Xin[1], LIU LiWu[2], ZHANG FengHua[1], LIU ZhengXian[2], WANG LinLin[1], LI QiFeng[2], PENG Fan[2], HAO SiDa[1], DAI WenXu[2], WAN Xue[1], TANG Yong[3], WANG Mian[3], HAO YanYan[3], YANG Yang[4], YANG Cheng[4], LIU YanJu[2] & LENG JinSong[1*]

[1] *Center for Composite Materials and Structures, Harbin Institute of Technology, Harbin 150080, China;*
[2] *Department of Aerospace Science and Mechanics, Harbin Institute of Technology, Harbin 150001, China;*
[3] *Institute of Telecommunication Satellite, China Academy of Space Technology, Beijing 100094, China;*
[4] *State Key Laboratory of Space Power-Sources Technology, Shanghai Institute of Space Power-Sources, Shanghai 200245, China*

With a 10% reversible compressive strain in more than 10 deformation cycles, the shape memory polymer composites (SMPCs) could be used for deployable structure and releasing mechanism. In this paper, without traditional electro-explosive devices or motors/controllers, the deployable SMPC flexible solar array system (SMPC-FSAS) is studied, developed, ground-based tested, and finally on-orbit validated. The epoxy-based SMPC is used for the rolling-out variable-stiffness beams as a structural frame as well as an actuator for the flexible blanket solar array. The releasing mechanism is primarily made of the cyanate-based SMPC, which has a high locking stiffness to withstand 50 g gravitational acceleration and a large unlocking displacement of 10 mm. The systematical mechanical and thermal qualification tests of the SMPC-FSAS flight hardware were performed, including sinusoidal sweeping vibration, shocking, acceleration, thermal equilibrium, thermal vacuum cycling, and thermal cycling test. The locking function of the SMPC releasing mechanisms was in normal when launching aboard the SJ20 Geostationary Satellite on 27 Dec., 2019. The SMPC-FSAS flight hardware successfully unlocked and deployed on 5 Jan., 2020 on geostationary orbit. The triggering signal of limit switches returned to ground at the 139 s upon heating, which indicated the successful unlocking function of SMPC releasing mechanisms. A pair of epoxy-based SMPC rolled variable-stiffness tubes, which clapped the flexible blanket solar array, slowly deployed and finally approached an approximate 100% shape recovery ratio within 60 s upon heating. The study and on-orbit successful validation of the SMPC-FSAS flight hardware could accelerate the related study and associated productions to be used for the next-generation releasing mechanisms as well as space deployable structures, such as new releasing mechanisms with low-shocking, testability and reusability, and ultra-large space deployable solar arrays.

shape memory polymer composite releasing mechanism, shape memory polymer composite tubes, flexible solar array

1 Introductions

At present, the spacecraft solar arrays usually undergo four steps, namely ground manufacturing-folding, collapsing-launching, space-space unfolding, and achieve orbit opera-tion [1]. The existing conventional rigid and semi-rigid panel solar arrays have a complicated structure, heavy weight and small area for deployment [2,3], which make it difficult to meet the power supply of next generation ultra-large space structures.

With the gradual maturity of new materials [4], especially for smart materials, the solar wing is currently developing in

---

the direction of simple structure, light weight, flexibility and ultra-large size [1–3]. As a new type of smart material, a shape memory polymer (SMP) can produce more than 100% of recoverable deformation under thermal stimulus [5–7]. A shape memory polymer composite (SMPC) combines the characteristic of large deformation of SMP and high stiffness of fiber reinforcement [8,9]. The SMPC has the following advantages: large deployment/storage rate; dual functions of structural loading and active deformation actuation, large damping, relatively slow deployment speed, and small impact during the unlocking and deployment process [10,11]. Therefore, the SMPC is a type of key structural material for large space deployable structures, especial for flexible solar arrays.

Deployable Space Systems, Inc. (DSS), conducted an on-orbit validation of the roll-out solar array (ROSA) in June 2017, funded by the U.S. Air Force, and successful achieved the space deployment of a flexible blanket solar array [12–15]. The ROSA was mainly made of conventional thin-wall composite tubes with "C" shape cross section [13,14]. This first in-space successful demonstration of the flexible solar array validated the deployment function, and structural dynamics properties in deployed configuration. The length of ROSA was 5.4 m long, and its fundamental frequency was around 0.4–0.5 Hz in bending mode [15]. Based on the ROSA's public data [12–15], an approximate estimation of the structural dynamics with various material strain limits is listed in Table 1. As shown in Table 1, as the maximum reversible strain of conventional fiber reinforced composite is around 2.0% [16–19], the maximum wall thickness of deployable structure is calculated to be approximate 0.2 mm, supposing that the curvature radius is 5 mm for the composite laminate during bending. According to the experience in the design of large solar arrays in recent years, the lowest fundamental frequencies should be no less than 0.2 Hz. Considering the above design limit, the limited length of the ROSA developed by DSS is estimated to be ~7.6 m. As a large-deformation and variable-stiffness material, the SMPC possesses a 10% reversible compressive strain in macro scale at the temperature above glass transition temperature (T_g), and meanwhile shows the same magnitude of stiffness as common fiber reinforced composites [20–23]. In this way, with the same forms of structure design as ROSA developed by DSS, the wall thickness of a composite laminate could increase from ~0.2 mm (ROSA) to ~0.6 mm (ROSA fabricated by SMPC, SMPC-ROSA) [22,23]. With the wall thickness 0.6 mm of SMPC, the limited length of supposed SMPC-FSAS could approach ~12.3 m with fundamental frequency ~0.4 Hz, and alternatively its limited length could also approach ~17.4 m with fundamental frequency of ~0.2 Hz. Based on the above approximate estimation, the SMPC shows great potential to be used for the ultra-large solar arrays compared with regular composites [24–26]. The

SMPC structures could significantly increase the stiffness and the associated fundamental frequency of the deployed space structures [27,28].

The space deployable structures need locking function during launching as well as releasing function on orbit. Currently, the traditional electro-explosive devices are used in most of cases for the locking and releasing. However, there are some disadvantages of the traditional electro-explosive devices: non-testability and non-reusability, high transient shocking during releasing process (~10000 g in ~0.02 s) [29,30]. With a 10% reversible compressive strain in more than 10 deformation cycles, the SMPC could be used for releasing mechanism with the function of testability and reusability. The duration of a deformation process upon heating stimulus is at a level of 10 s, and thus the shocking of SMPC releasing mechanism is closed to zero when unlocking [31,32]. Therefore, the SMPC shows the potential to be used for releasing mechanism in aerospace.

Based on our previous study in on-orbit validation of SMPC in material-level [33] and part-level [34], the rollable SMPC flexible solar array system (SMPC-FSAS) in system-level is studied, developed, ground-based tested, and on-orbit validated. An epoxy-based SMPC is proposed to be used for the rolling-out variable-stiffness beams as the frame for a flexible blanket solar array, and a cyanate-based SMPC is used for the releasing mechanism. This project was administered by Institute of Telecommunication Satellite, China Academy of Space Technology (CAST).

2   Structural design and analysis of the SMPC-FSAS

2.1   Design of the flexible solar array system

On the basis of SMPC, the SMPC-FSAS is mainly made of a pair of SMPC rolling-out variable-stiffness tubes with lenticular cross section, one piece of flexible blanket solar array clapped between the two SMPC tubes, and the SMPC releasing mechanisms. As shown in Figure 1 and Table 1, the main components of the SMPC-FSAS are included as follows: (1) One pair of SMPC rollable variable-stiffness tubes (I) with lenticular cross section. They were made of epoxy-based SMP reinforced by carbon twill weaves. They can deploy by electrical heating upon applying a direct current on the resistive heating films which are attached on the both outer surfaces of the SMPC tubes, and they can also provide a relatively high structural stiffness for the solar array in deployed plane state in space. (2) Flexible blanket solar array (II). It is can be deployed from a stowed rolled state to the deployed plane state for solar power production, and the actuation force is generated from the stored strain energy in SMPC and trigged by the temperature. Due to the one-way effect of SMP, the deployed configuration of flexible blanket

Table 1 Approximate estimation of the structural dynamics based on the ROSA's public parameters (supposed curvature radius 5 mm of the composite laminate during bending)

	Maximum strain	Wall thickness of a composite laminate (mm)	Length of a beam (m)	Frequency of a beam (Hz)
ROSA developed by DSS	2%	0.2	5.4	0.4
	2%	0.2	~7.6	~0.2
Supposed SMPC-ROSA	10%	~0.6 [a]	~12.3	~0.4
	10%	~0.6 [a]	~17.4	~0.2

a) The calculation method is referred to refs. [20–23].

solar array can be kept even if the temperature is higher than the T_g of SMP. (3) One pair of SMPC releasing mechanisms (III). They were made of cyanate-based SMP reinforced by carbon twill weave. They lock the flexible blanket solar array in rolled configuration with a high locking structural stiffness. When heating above their T_g through electrical heating the resistive films attached on the both surfaces of the SMPC laminates, the SMPC contract and therefore release the rolled flexible solar array. Note that, the so-called flexible solar array system contains I (SMPC rollable variable-stiffness tubes) and II (flexible blanket solar array).

The key structural parameters of SMPC-FSAS (Figure 2 and Table 2) are: folded envelope size 420 mm×200 mm ×85 mm, deployed envelope size 420 mm×200 mm ×338 mm, total weight 1.88 kg, weight for rolling-out components around 0.22 kg. According to structural design of the SMPC-FSAS, the main resource supplied from the satellite include the electrical power supply for resistive heating the SMPC, the telemetry interface for testing the temperature and limit switch indication, and analog channel for the voltage indication of solar array. The detailed resources given by
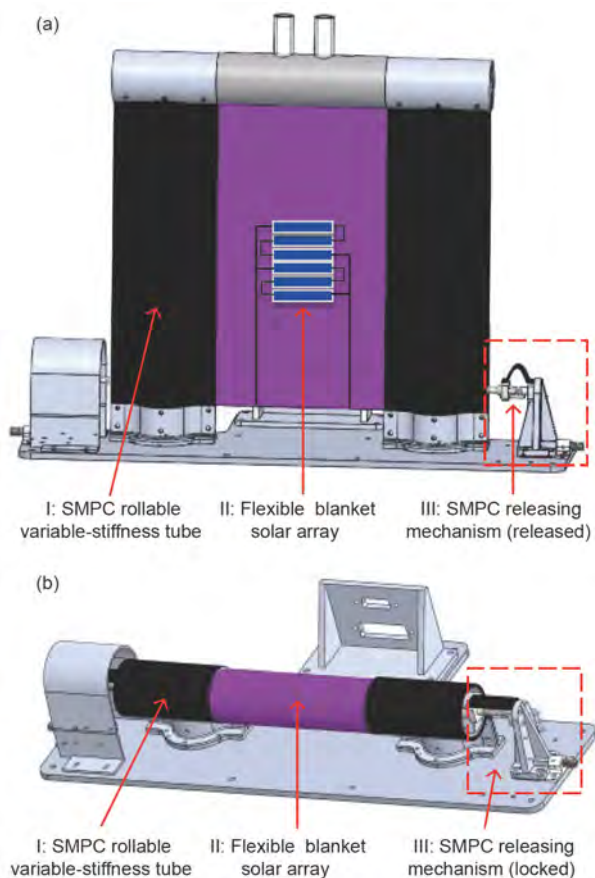

Figure 1 Structural design of SMPC-FSAS aboard the SJ20 Geostationary Satellite. (a) Deployed state; (b) folded state.
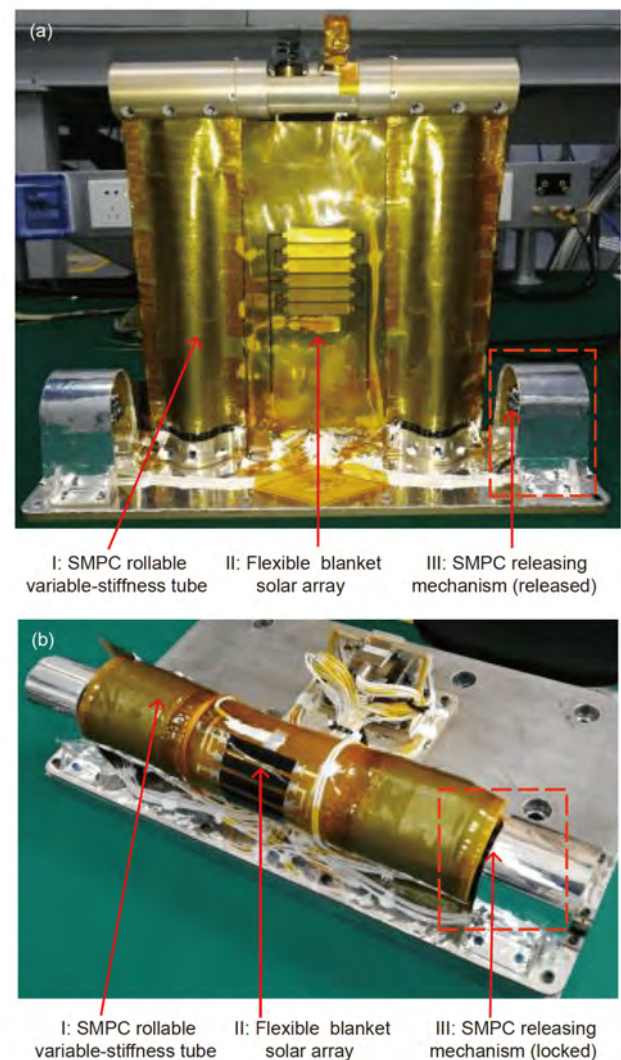

Figure 2 SMPC-FSAS flight hardware for on-orbit evaluation aboard the SJ20 Geostationary Satellite. (a) Deployed state; (b) folded state.

Table 2   Key parameters of design and performance of SMPC-FSAS aboard the SJ20 Geostationary Satellite

Items	Value
Mass	1.88 kg
Folded outermost size	420 mm×200 mm×96 mm
Deployment outermost size	420 mm×200 mm×338 mm
Signal testing channels	Seven channels of telemetry interfaces: six channels for temperature, one channel for limit switch
Power supply of satellite	One channel of 100 V/80 W, two channels of 100 V/180 W
Power of SMPC-FSAS	SMPC releasing mechanism 4.2 W (100 V/80 W from satellite), SMPC rollable beam 80 W (100 V/180 W from satellite), SMPC rollable beam and additional devices 74 W/Ω (100 V/180 W from satellite)
Fundamental frequency in a deployed state	21.97 Hz
Deployment duration	Total duration of deployment ~6 min SMPC releasing mechanism, ~4 min SMPC rollable beam, ~2 min
T_g	Cyanate-based SMPC of releasing mechanism, 210°C Epoxy-based SMPC of SMPC rollable beam, 150°C
Displacement of SMPC pin pullers of releasing mechanism	Releasing displacement of rollable beams, 4 mm Triggering displacement for limit switches, 7 mm Unconstrained ultimate displacement, 10 mm
Shape recovery ratio	SMPC rollable beam, 100%
Design life span	1 year for releasing mechanism; 5 years for SMPC rollable beam in deployed sate

satellite for SMPC-FSAS are included as follows: (1) one channel of 100 V/80 W direct current (DC) circuit for resistive heating the curved SMPC laminate of the two releasing mechanisms, with the aim to release the rolled flexible solar array. (2) Two channels of 100 V/180 W DC circuits for resistive heating the two rolled SMPC tubes with lenticular cross sections. (3) Seven channels of telemetry interfaces for temperature signal monitoring (six channels) and limit switches indication (one channel) for the SMPC-FSAS. (4) One analog channel to measure the output voltage of the flexible solar array in space.

As a deployment device installed on a geostationary satellite, the various requirements of satellite should also be considered, including structure design and various interfaces: (1) Mechanical interface. The SMPC-FSAS was installed through punching 12 holes on the outside of the east deck of satellite. The metallic base of the SMPC-FSAS was used to connect the satellite deck by screws with installation aperture 4.5±0.1 mm, flatness 0.1 mm/100 mm×100 mm, and the roughness was 3.2 μm. (2) Thermal interface. The SMPC-FSAS was installed outside the satellite cabin, and its temperature range of the satellite deck was 0°C–50°C. (3) Reliability. According to the reliability standard GB/T 7826-1987, a reliability model should be established, considering the releasing mechanism and deployment process. The reliability of the SMPC-FSAS at the end of its life period should be greater than 0.94. (4) Radiation resistance. The SMPC-FSAS should meet the 5-year life span within geos-

tationary irradiation environment. (5) Electrical connection. The electrical installation of the SMPC-FSAS should meet the following requirements: the product base plate achieves effective electrical overlap and mechanical fixation with the satellite grounding system, and the DC resistance does not exceed 10 mΩ. (6) Electromagnetic compatibility: None. (7) Life span. The overall design of SMPC-FSAS was more than 1 year in the stowed state and more than 5 years in the deployed state.

Different with shape memory alloy (SMA), the SMP is a molecular plastic. The current SMP in this paper only shows the one-way shape memory effect. That is, after deployment, the external force has to be applied to the SMP (in soft state above T_g) to conduct the second shape memory cycle. For the flexible blanket solar array, it is can be deployed from a stowed rolled state to the deployed flat state for solar power production, and the actuation force is generated from the stored strain energy in SMPC and trigged by the temperature. Due to the one-way effect of SMP, the deployed flat configuration of flexible blanket solar array can be kept even if the atmosphere temperature is higher than the T_g of SMP.

The epoxy-based SMPC of rollable beam has been systematically characterized in our previous paper [34] as a basic technical supporting for this current project. The T_g of epoxy-based SMPC was 150°C. In addition, the T_g of cyanate-based SMPC of releasing mechanism was 210°C. The materials, mechanics, structure design and experimental evaluation of cyanate-based SMPC will be studied in a future

paper, which will specially discuss the SMPC releasing mechanism.

2.2   SMPC releasing mechanism

The SMPC releasing mechanism is used to lock the rolled flexible solar array, and also release it upon heating. It mainly consists of SMPC laminates, metallic springs, metallic pin pullers, limit switches for releasing indication and frame. As shown in Figure 3(a), the SMPC laminate was initially solidified into a curved "Ω" shape in an oven, and then pre-deformed into extended flat shape (Figure 3(a-1)) with external force, and finally installed onto the releasing mechanism to supply an adequate preload through pin puller to lock the rolled solar array. In particular, there are two pin pullers (Figure 3(a-3)) to apply proper force on both sides of a hollow cylinder which is connected with the tips of both epoxy-based SMPC tubes. For each pin puller, one end is connected to the cyanate-based SMPC laminate, and there is a conical plug on its other end to insert into the groove of the hollow cylinder for preloading. Meanwhile, the metallic spring of the releasing mechanism is in a pre-stretching state. In this way, the rolled flexible solar array is locked by the SMPC releasing mechanism (Figure 3(a-2), (a-3)). As shown in Figure 3(b), during the releasing procedure, upon heating the resistive films attached on the both sides of SMPC planar

laminate, it will recover from flat shape to the curved "Ω" shape (Figure 3(b-1)), which will pull the pin puller out of the groove of the hollow cylinder. In this way, the rolled flexible solar array is released (Figure 3(b-2), (b-3)).

Considering the mechanics design of the preload to lock the stowed solar array, the locking stiffness of releasing mechanism should be adequate to restrain the movable parts of solar array with a total mass of around 0.21 kg. The movable parts include two cantilever SMPC variable-stiffness tubes, flexible blanket solar array, hollow cylinder parts connected at the two tips of the cantilever SMPC tubes, and the wires. The maximum vibration acceleration applying on the SMPC-FSAS is estimated to be 15 g during launching of Long-March-5 Y3 Heavy Rocket. The preload of releasing mechanism is designed to withstand 50 g gravitational acceleration with a factor of safety 2.33. The dimensions of flat SMPC laminate were 38 mm length, 21 mm width and 2 mm thickness, and the length of SMPC laminate in released state ("Ω" shape) was 28 mm. The stiffness coefficient of metallic spring was 1500 N/m. The length of metallic spring in a free state was 26 mm, and it was 36 mm in the pre-stretched locking state with the pre-tensioning force 15 N. With the above design margin, the according locking preload is calculated to be 106.5 N (SMPC laminate: 121.5 N, spring: −15 N) based on the mass of locking object, namely the 0.21 kg of movable parts. In addition, during the reality
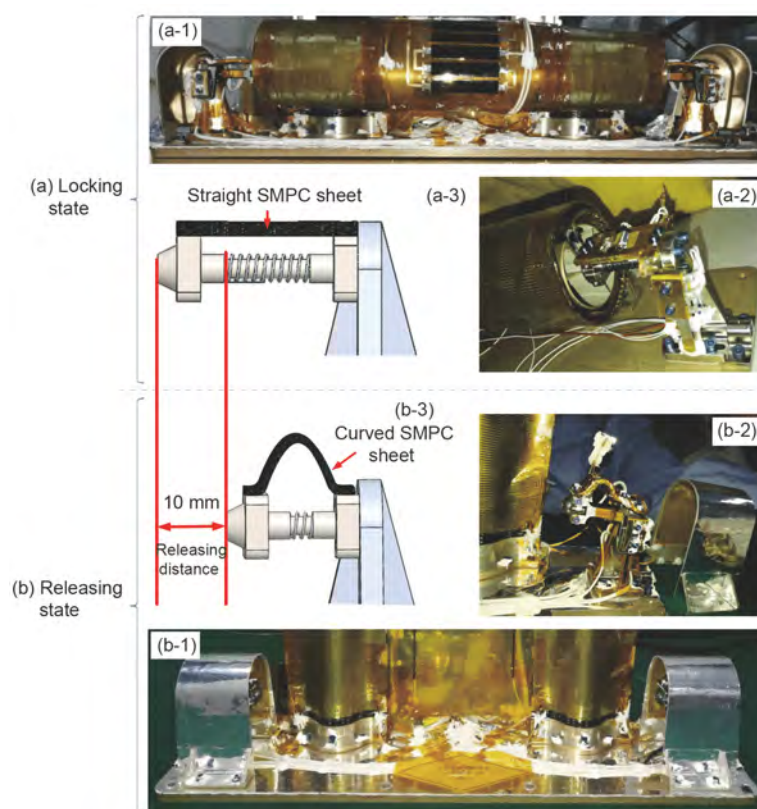

Figure 3   SMPC releasing mechanism flight hardware of SMPC-FSAS aboard the SJ20 Geostationary Satellite.

process of assemble of flight hardware, the transverse pre-tensioning force of pin puller was projected to be 138 N (SMPC laminate: 153 N, spring: −15 N) with the associated pre-tensioning moment 0.8 N m of screw. In this way, the actual factor of safety is 3.38, which is adequate to ensure the safety for locking during the launching process of rocket. In addition, in order to evaluate the stiffness of the SMPC releasing laminate, the compression test was conducted along the longitudinal direction. Two ambient temperatures were employed: the room temperature (20°C) and 83°C. The extremely-high temperature 83°C was deviated by 30°C on the basis of the result of thermal equilibrium test result of 53°C. Figure 4 indicated the compressive force versus displacement of the flat SMPC laminate at 20°C and 83°C. Below the load of 153 N, the curves of 20°C and 83°C also show a relative good linearity with a compressive displacement of 0.1–0.2 mm, which shows a relative high compressive stiffness of the SMPC laminate. The compression test shown in Figure 4 was conducted along the longitudinal direction of SMPC laminate, which was consistent with direction of pre-tensioning force of the flat SMPC laminate of releasing mechanism in a locked state.

As an important component part of releasing mechanism, the cyanate-based SMPC laminate possesses a high transition temperature (T_g=210°C) to ensure the reliability of locking function in possible high temperature ambient environment on geostationary orbit. When heated, the flat SMPC laminate recovered into curved configuration, and meanwhile pulled the associated pin puller to gradually separate from the rolled solar array. When the lateral displacement of pin puller approached 4 mm, the hollow cylinder at the tip of rolled solar array was completely free. In addition, two limit switches were installed on the releasing mechanisms to indicate the state of releasing. When the lateral displacement of pin puller approached 7 mm, the limit switches were triggered. The maximum lateral movement displacement of pin puller was 10 mm to ensure the safety margin for reliable triggering as shown in Figure 3(b).

In addition, the pre-tensioning mechanism included a regulating screw, a pre-tensioning base, and a support. The pre-tightening mechanism achieved pre-tightening force by adjusting the regulating screw. One end of the regulating screw was pressed against the groove of the support, and the length of the regulating screw was adjusted by screw holes on both sides of the pre-tensioning base. The hollow cylinder, with a diameter of 40 mm, played the role of rolling and fixing the flexible blanket solar array. There was a clamping groove along the diameter direction, which was used to fix the end of the solar array. On both sides of the hollow cylinder, there were cone grooves for locking pins, which were used to connect the locking pins to achieve the function of locking and fixing. In this way, the flexible blanket solar array can be rolled along the outer surface of hollow cylin-
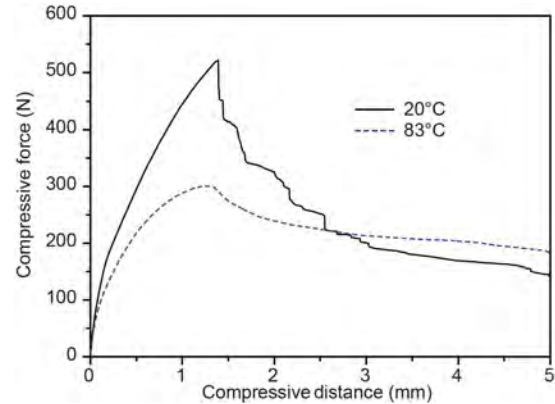

Figure 4 (Color online) Force versus displacement curves of the flat SMPC laminate at 20°C and 83°C.

der, and meanwhile fixed by the releasing mechanism installed on the base of SMPC-FSAS.

The metallic spring was still in the stretched state when the SMPC laminate recovered from flat shape to the curved "Ω" shape. The total pre-stretched distance of metallic spring was 10 mm. When released, the displacement of the conical plug of releasing mechanism was 7 mm. Therefore, the total pre-stretched distance of metallic spring was 10 mm. When released, the displacement of the conical plug of releasing mechanism was 7 mm. Therefore, the pre-tensioning force of metallic spring was 4.5 N (i.e., 1500 N/m×3 mm). The releasing process of the SMPC releasing mechanism was a combinational behavior with SMPC and metallic spring. The design, manufacture and characterization will be discussed in details in a future paper.

2.3 SMPC rollable variable-stiffness tubes

As shown in Figure 5, there is one pair of SMPC rollable variable-stiffness tubes, which are used to fix the flexible blanket solar array, the polyimide-based SMP film, and the hollow cylinder on their tips. The cross section of SMPC tube is lenticular to allow a relatively high structural stiffness in a deployed shape, as well as allow a relatively low material strain as the two curved laminates deformed into planar state and contact with each other in a rolled shape. The shape memory materiel is an epoxy-based SMP reinforced by carbon twill weaves. The T_g of this SMPC is around 150°C. This SMPC with thickness of 0.4 mm allows a relatively high recovery forces during deployment process. The recovery ratio of this lenticular SMPC is around 100% because that the structural stable state can be only achieved once straight. Regarding the component parts of SMPC tubes, a clamping part and inner core are used to fix the SMPC tubes onto the base of SMPC-FSAS. The clamping parts, inner core and SMPC tubes are connected by bolts. The shape recovery ratio can approach at 100% during the shape recovery test at 25°C ambient environment in air (Figure 6).

Figure 5 (Color online) The design of SMPC variable-stiffness tubes with lenticular cross section. (a) Folded state; (b) deployed state.
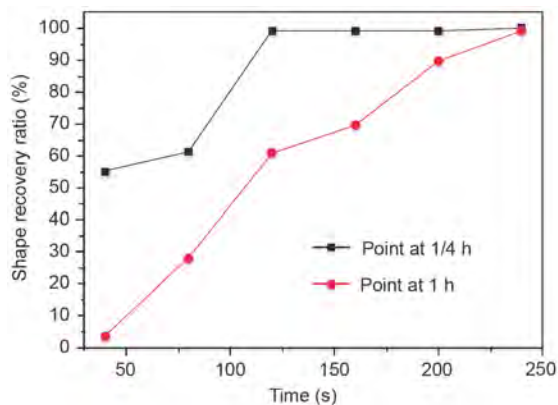

Figure 6 (Color online) Shape recovery ratio of the SMPC variable-stiffness tube with the indicating points at the position of 1/4 h (closed to the bottom of the tube) and 1 h (at the tip of tube).

Our previous study [34] has discussed the related design, simulation, and experimental evaluation for the SMPC tubes with lenticular cross section.

2.4 Flexible blanket solar array

The assembly of blanket flexible solar array was made of gallium arsenide solar cells, which was specially researched and developed by State Key Laboratory of Space Power-Sources Technology for this space experiment mission. Its dimension was 150 mm×260 mm. It was fixed by clamping between the two SMPC shells and adherent by epoxy-resin during the second-solidification, with the overlapping area with the SMPC tubes of 10 mm×150 mm. During the rolling process, the flexible blanket solar array was rolled and tightly pressed around the hollow cylinder. During the deployment process, they unfold together with the SMPC tubes. Note that, as the main purpose of the project was to

study and validate the releasing and deployment functions of smart structure based on SMPC materials, the power production of the flexible blanket solar array was not discussed in details in this paper.

3 Ground-based tests of the SMPC-FSAS

As a spaceflight hardware production, the mechanical reliability of the SMPC-FSAS should be critical considered and examined through the ground-based testing before launch. Considering all the components of the SMPC-FSAS, they include a pair of SMPC rolling-out variable-stiffness tubes, one piece of flexible blanket solar array, a pair of SMPC releasing mechanisms, the metallic base, thermocouples, limit switches, various resistive heating films, various wires, electrical connectors, silicone rubber, and various screws. The ground-based tests of mechanical reliability for all the components of SMPC-FSAS include structural dynamics performance, thermal performance, and releasing and deployment evaluation. All the ground-based testing procedures strictly followed the related demands of China aerospace standards for flight hardware of acceptance level.

3.1 Structural dynamics performance tests

In order to ensure the dynamics performance of SMPC-FSAS, structural dynamics testing are required, including sinusoidal sweeping and random vibration test (stowed state), shocking test (stowed state), acceleration test (stowed state) and sinusoidal sweep vibration test (deployed state). During the testing, the electronic components were shortly powered on to monitor sensitive parameters for possible faults. Before and after each test, the extrinsic appearance of all the components was checked. All the dynamics tests cover three directions, one of which was perpendicular to the mounting base plate (Z direction), and the other two directions were parallel to the mounting base plate (X direction and Y direction).

3.1.1 Sinusoidal sweeping vibration test and random vibration test (stowed state)

Sinusoidal sweeping vibration test and random vibration test were both carried out on a M1216VH electric vibration table, as shown in Figure 7. An accelerometer was mounted on the SMPC tube structure to collect vibration relevant data. The resistance of the resistive heating film was measured before and after the test to check whether it was damaged. The vibration process was recorded, and the structure was checked after each test. For the testing parameters of sinusoidal sweeping vibration, the acceleration is specified into 10 g in all the three directions with sweeping rate of 4 oct/min. For the random vibration testing, the acceleration
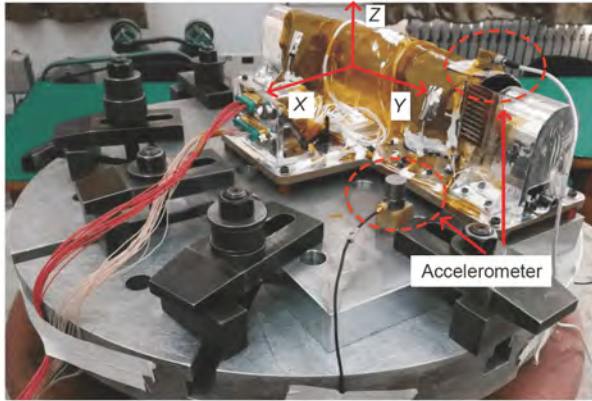
Figure 7 (Color online) Sinusoidal sweeping vibration test and random vibration test in *Z* direction.
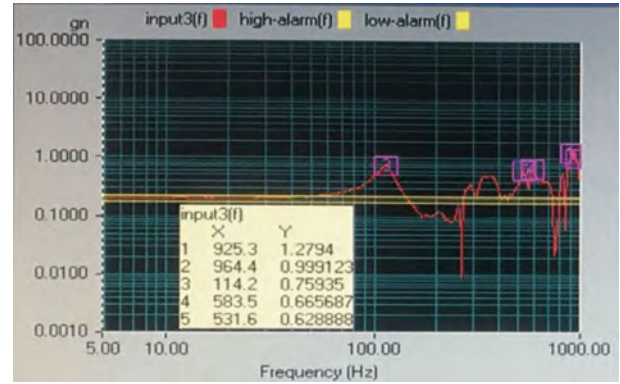

Figure 8 (Color online) Frequency response of characteristic sinusoidal sweeping vibration test (0.2 g) in *Z* direction after random vibration for SMPC-FSAS in stowed state.

(total root mean square) were 10.2 g for *X* and *Y* directions, and 13.2 g for *Z* direction with testing duration 1 min in each direction. In addition, the characteristic sweeping test was carried out before and after each vibration testing, namely totally three tests in each direction (before sine sweeping, after sine sweeping and after random vibration). The range of characteristic sweeping test was 5–1000 Hz with 0.2 g acceleration and 4 oct/min sweeping rate.

For the test in *X* direction, the testing was conducted with the following testing items in sequence: (1) characteristic sweep (0.2 g); (2) sinusoidal sweeping (10 g); (3) characteristic sweep (0.2 g); (4) random vibration (10.2 g); (5) characteristic sweep (0.2 g). The resulted data of frequency response of characteristic sweeping in *X* direction are listed in Table 3, including natural fundamental frequencies and the corresponding responses of acceleration amplitudes. Without any other treatment after testing in *X* direction, the tests in *Y* direction and in *Z* direction were continuously conducted in sequence, and the corresponding results are listed in Table 3. The results show that the natural frequencies shift less than 1% in most cases after experiencing sinusoidal sweeping vibration (10 g) as well as random vibration (10.2 g or

13.2 g), indicating that the locking stiffness of releasing mechanism behaves relatively stable. When examining its safety during launching aboard the rocket, the natural frequencies of the SMPC-FSAS in certain direction are selected by authors using the results of characteristic sweeping after random vibration test. In this way, the natural frequencies in *X* direction are 123.39, 204.98, and 294.56 Hz. They are 126.63, 260.17, and 416.74 Hz in *Y* direction, and 114.20, 531.60, and 583.50 Hz in *Z* direction, respectively. Naturally, the lowest natural frequency is at the *Z* direction (114.20 Hz) as shown in Figure 8, because that the plane of SMPC laminate in locking state is located at the *X*-*Y* plane and the according structural stiffness in *Z* direction is lower than those in *X* and *Y* directions. In addition, the acceleration responses in each direction also show consistence. In special, the dynamic magnification factor is around 4 (0.8 g/0.2 g=4) in *Z* direction which is also due to the relatively low structural stiffness of SMPC laminate in *Z* direction of the releasing mechanism.

3.1.2 Shocking test (stowed state)

The shocking test of the SMPC-FSAS was carried out on the

Table 3 Frequency response of characteristic sinusoidal sweeping vibration test (0.2 g) for SMPC-FSAS in stowed state [a]

	Before sine sweeping		After sine sweeping		After random vibration	
	Freq. (Hz)	Acce. (g)	Freq. (Hz)	Acce. (g)	Freq. (Hz)	Acce. (g)
X direction	120.23	0.487	120.24	0.461	123.39	0.512
	204.98	1.031	204.98	1.059	204.98	1.132
	293.03	1.794	293.03	1.849	294.56	1.785
Y direction	127.95	0.299	126.63	0.286	126.63	0.288
	258.78	0.500	260.13	0.493	260.17	0.491
	416.74	1.043	416.74	1.040	416.74	0.996
Z direction	114.20	0.949	113.60	0.801	114.20	0.759
	528.90	0.542	531.60	0.571	531.60	0.629
	896.90	0.609	901.60	0.629	583.50	0.666

a) Freq.: natural frequency; Acce.: amplitude of acceleration.

CXP-100 shock-response testing machine. During testing, relevant data were collected and the video was recorded. After each test, all the structural appearance was inspection. The shocking testing parameters: frequency +6 dB/oct (100–1500 Hz), 800 g (1500–4000 Hz), one testing for each direction (*X*, *Y*, and *Z* directions). Figure 9 shows the impact test setup of the SMPC-FSAS. After the shocking testing in three directions, all the sensitive components (thermo-couples, resistive heating film, limit switches, etc.) were carefully checked, and they all worked in normal. No faults or failures was found for the appearance of SMPC-FSAS.

3.1.3 Acceleration test (stowed state)

The acceleration test was performed using the 43-type acceleration centrifuge (Figure 10). The magnitude of acceleration testing was 10 g. The test was carried out in three directions, namely *X*, *Y*, and *Z*, respectively. The holding time was 5 min for each direction, and the loading rate was ≤5 g/min. Video was recorded during the testing to observe whether the structure was damaged. The resistance of the
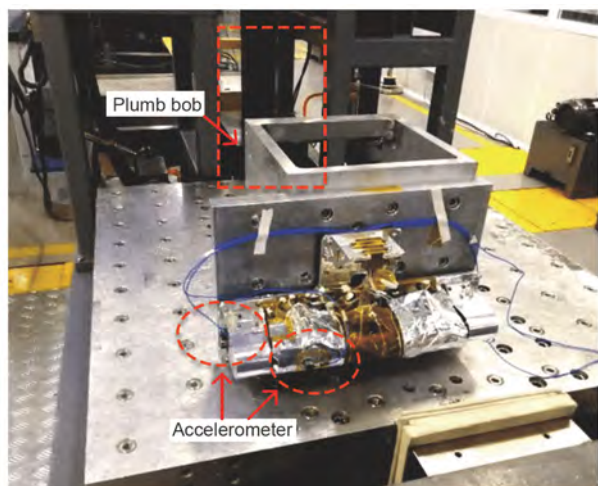
heating films was measured before and after testing in each direction. After the acceleration testing in three directions, all the sensitive components (thermocouples, resistive heating film, and limit switches) were also checked carefully, and they all worked in normal. No faults or failures was found for the appearance of SMPC-FSAS.

3.1.4 Sinusoidal sweeping vibration test (deployed state)

In order to ensure the safety of the SMPC-FSAS in deployed configuration, its deployed structural dynamics behavior needs to be tested. The natural frequencies of the SMPC-FSAS in deployed configuration were mainly tested through characteristic sweeping sinusoidal vibration test in all the three directions (Figure 11). Accelerometers were mounted on the hollow cylinder to collect vibration response data. The range of characteristic sweeping test is 5–1000 Hz with 0.2 g acceleration and 4 oct/min sweeping rate. The testing process was recorded by video. The structure appearance was checked after each experiment.

The frequency responses in three directions were tested. The fundamental frequency of the deployed structure in *X* direction is 21.97 Hz as shown in Figure 12. The corresponding amplitude of acceleration response is 4.26 g, with the dynamic magnification factor is 21.3 (4.26 g/0.2 g=21.3) in *X* direction. Accordingly, the fundamental frequencies in *Y* and *Z* directions are 104.98 and 439.45 Hz, respectively. The dynamic magnification factors in *Y* and *Z* directions are 47.8
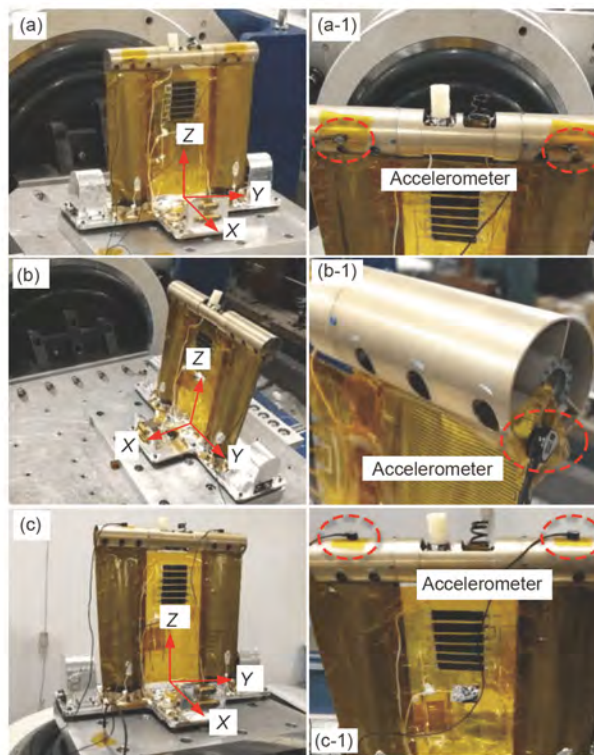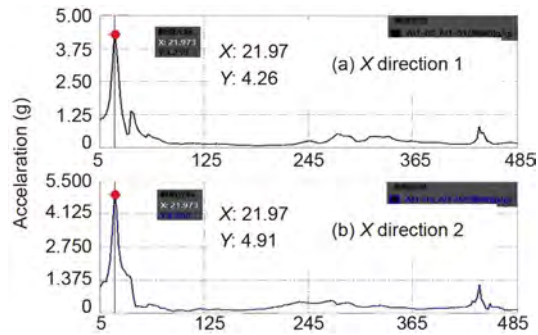
Figure 12 (Color online) Frequency response curves of 0.2 g characteristic sinusoidal sweeping vibration test of the SMPC-FSAS in deployed state.

(9.56 g/0.2 g=47.8), and 75.05 (15.01/0.2=75.05), respectively. Considering the results in the three directions, the fundamental frequency in *X* direction (21 Hz) is the lowest one, because that the SMPC tubes in *X* direction shows the lower stiffness than those in *Y* or *Z* directions. The fundamental frequency of 21 Hz of the SMPC-FSAS is high enough for a deployed structure in space, where it is as low as around 0.2 Hz for many deployed flexible solar array system in large scale. The appearance of all the components was checked after vibration tests.

3.2 Thermal performance tests

In order to ensure the stability and reliability of SMPC-FSAS when exposed to on-orbit ambient environments, the systematical evaluation of hot and cold temperature extremes were performed, including thermal equilibrium test (steady-state and transit-state), thermal vacuum cycling test (6.5 cycles), and thermal cycling test in air (18.5 cycles).

3.2.1 Thermal equilibrium test

In order to accurately predict the temperature of different orbital positions and different parts of SMPC-FSAS in stowed state on orbit, thermal equilibrium tests of steady state and transient state were performed. In addition, the results of the thermal equilibrium test also provided a reference temperature for subsequent thermal vacuum cycling and thermal cycling in air. As the SMPC-FSAS was mounted on the east deck of SJ20 geosynchronous orbit satellite, the temperature change of SMPC-FSAS on orbit has a period of 24 h. The thermal equilibrium test of the SMPC-FSAS was performed using the solar simulator as shown in Figure 13. Primary operating parameters included vacuum degree $\leq 1.35 \times 10^{-3}$ Pa, cold black screen temperature 100 K. Ten units of multilayer with the outermost yellow layer film were laid on the simulated plate to simulate the deck of satellite. Twelve round holes were opened in the multilayer, and polyimide insulation pads (10 mm in diameter) were placed in the 12 round holes. The SMPC-FSAS was mounted onto
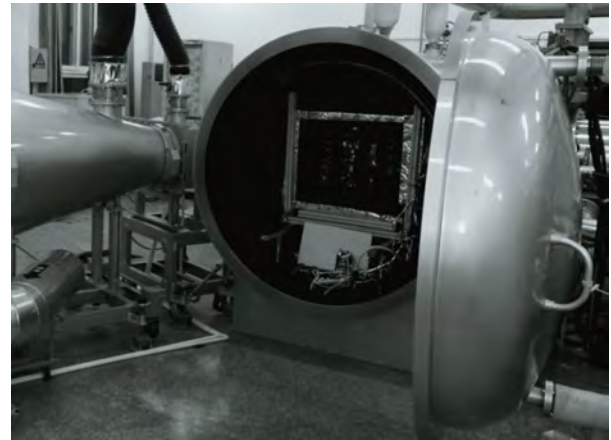

Figure 13 Thermal equilibrium test: solar simulator and the SMPC-FSAS flight hardware mounted on the simulated plate.

the simulated plate through the insulation pads. The irradiation direction of solar simulator is perpendicular to the mounting plate.

The steady-state thermal equilibrium test under high-temperature conditions was to evaluate the temperature distribution of SMPC-FSAS under the possible extreme high-temperature conditions (equivalent to 90° incident direction of sunlight at 12 o'clock) in long term. It started from the maximum heat flow in high-temperature condition (1 solar constant, 1414 W/m^2) to simulate the 12 o'clock noon condition. The criterion for reaching steady-state thermal equilibrium under high-temperature conditions was that the value of monotonic change was no greater than 0.1°C/h within continuous 4 h. The temperature of the simulated plate was adjusted to be ~45°C by heating the resistive films attached. The extremely-high temperature of steady-state thermal equilibrium can be obtained through this test.

The transient thermal equilibrium test aimed to accurately predict the temperature change of SMPC-FSAS within a 24 h period of a day, especially for the high temperature with 90° incident direction of sunlight as well as the deep low temperature under no-light conditions at night. The heat flow with the step values is listed in Table 4. The testing of extremely-high temperature of transient state starts from the high temperature steady state process in order to obtain the extreme high temperature transient temperature within 24 h. The extremely-high temperature and extremely-low temperature transient-state thermal equilibrium could be obtained through this test. In order to comprehensively monitor the distributions of temperature, totally 18 thermocouples (simplified as TH1–TH18) were mounted on the SMPC-FSAS (see Table 5) during steady-state thermal equilibrium test and the transient thermal equilibrium test.

The steady-state thermal equilibrium was realized with the heat flow 1414 W/m^2 of solar simulator. Table 5 lists the summarized results for extremely-high temperatures of steady-state thermal equilibrium. They are different de-

Table 4 Step values of the heat flow of transient thermal equilibrium test

Test time (h)	Simulated time on orbit	Incident angle (°)	Heat flow (W/m^2)	Temperature of simulated plate (°C)
0–1	13:00–14:00	105	1365.82	
1–2	14:00–15:00	120	1224.56	
2–3	15:00–16:00	135	999.85	50
3–4	16:00–17:00	150	707.00	
4–5	17:00–18:00	165	707.00 [a]	
5–17	18:00–6:00 (the next day)	/	0	−10
17–18	6:00–7:00	0	707.00 [a]	
18–19	7:00–8:00	15	707.00 [a]	
19–20	8:00–9:00	30	707.00	
20–21	9:00–10:00	45	999.85	50
21–22	10:00–11:00	60	1224.56	
22–23	11:00–12:00	75	1365.82	
23–24	12:00–13:00	90	1414.00	

a) As the minimum output power of the solar simulator is 700 W/m^2, the actual power 707 W/m^2 was taken when the calculated powder was lower than 707 W/m^2.

Table 5 Extremely-high temperatures of steady-state and transient-state thermal equilibrium tests of the SMPC-FSAS (temperature points from TH1 to TH18)

Number of thermocouples	Locations of thermocouples	Extremely-high temperature of steady-state thermal equilibrium (°C)	Extremely-high temperature of transient-state thermal equilibrium (°C)
TH1	lens hood 1, +Z	30.65	28.37
TH2	lens hood 1, +X	31.47	29.19
TH3	lens hood 2, +Z	12.86	11.00
TH4	lens hood 1, +X	12.10	10.15
TH5	Base of SMPC-FSAS	49.55	48.02
TH6	Cyanate-based SMPC locking laminate 1 of releasing mechanism, +Z (SMPC deformation area, no light)	37.84	34.81
TH7	Cyanate-based SMPC locking laminate 1 of releasing mechanism, +Z (exposed to light)	46.92	43.59
TH8	Cyanate-based SMPC locking laminate 2 of releasing mechanism, +Z (SMPC deformation area, no light)	29.19	26.72
TH9	Cyanate-based SMPC locking laminate 2 of releasing mechanism, +Z (exposed to light)	53.09	50.38
TH10	Epoxy-based SMPC tubes 1, +X	30.08	29.08
TH11	Epoxy-based SMPC tubes 1, +Z	68.94	68.66
TH12	Epoxy-based SMPC tubes 1, −X	28.57	26.72
TH13	Epoxy-based SMPC tubes 2, +X	37.01	35.66
TH14	Epoxy-based SMPC tubes 2, +Z	73.23	72.06
TH15	Epoxy-based SMPC tubes 2, −X	35.83	34.24
TH16	Flexible solar array, +X	39.45	38.25
TH17	Flexible solar array, +Z	42.49	40.98
TH18	Flexible solar array, −X	33.53	32.06

pended on the locations. The extremely-high temperatures on the top of two epoxy-based SMPC tubes of solar array are 68.94°C (TH11) and 73.23°C (TH14), respectively. The temperatures at deformation area of the two cyanate-based SMPC laminates of releasing mechanisms are 37.84°C (TH6) and 29.19°C (TH8), respectively. The highest tem-

perature is 73.23°C (TH14), which appears on the epoxy-based SMPC tubes.

For the transient temperature test, the structure experienced a hot-cold-hot cycle in a vacuum tank to simulate 1-day heat flow. Figure 14 and Table 5 show the temperatures of transient-state thermal equilibrium. Similar with the re-
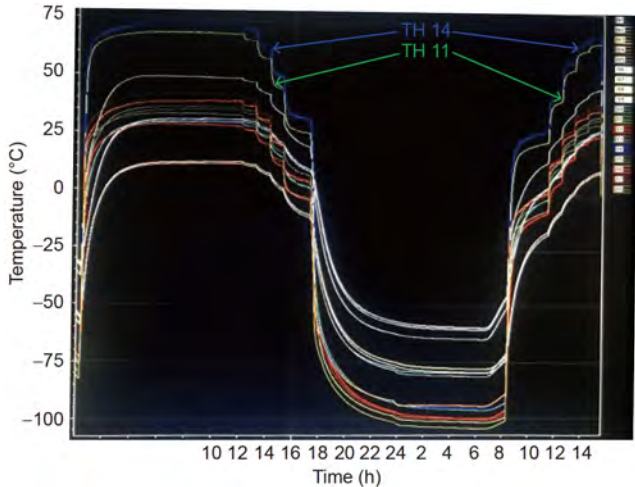
Figure 14 (Color online) Temperature curves of the transient-state thermal equilibrium of the SMPC-FSAS (temperature points from TH1 to TH18).

sults of steady-state thermal equilibrium test, the extremely-high temperature of the transient thermal equilibrium test is 72.06°C (TH14), which also appears on the epoxy-based SMPC tubes. The temperatures of the transient thermal equilibrium test on the top of two epoxy-based SMPC tubes of solar array are 68.66°C (TH11) and 72.06°C (TH14), respectively. The temperatures at deformation area of the two cyanate-based SMPC laminates of releasing mechanisms are 34.81°C (TH6) and 26.72°C (TH8), respectively.

As shown in Table 5, the temperatures of the steady-state thermal equilibrium tests are coincident well with those of transient-state thermal equilibrium tests at the same points, which indicates that the heat capacity of the SMPC-FSAS is low and it is quick to reach the thermal steady state. As shown in Table 6, based on the thermal equilibrium tests, the extremely-high temperature of SMPC-FSAS is at the top of epoxy-based SMPC tubes (72°C–73°C), and the extremely-high temperature of SMPC laminate of releasing mechanism is 26°C–35°C. The extremely-low temperature of SMPC-FSAS is lower than −70°C.

In order to ensure the reliability in engineering applications, the reference high temperature for thermal vacuum test and thermal cycle test was selected as 73°C, and the reference low temperature was selected as −102°C.

3.2.2 Thermal vacuum cycling test

In order to verify the structural and functional characteristics of SMPC-FSAS on orbit after long-term exposure to thermal vacuum conditions, a thermal vacuum cycling test was conducted as shown in Figure 15. Based on the results of the thermal equilibrium test (reference high temperature 73°C, reference low temperature −102°C), the extremely-high temperature and extremely-low temperature of the thermal vacuum cycle tests were deviated by 15°C. Therefore, the low temperature limit of the thermal vacuum cycle test was set at 88°C, and the high temperature limit was set at 117°C.

Figure 15 shows the setup of SMPC-FSAS for the thermal vacuum test in space environment simulation equipment (KM2). The total number of thermal vacuum cycles was 6.5. The environmental pressure of the thermal vacuum in tank was 6.8×10^{-4}–4.2×10^{-4} Pa. In each thermal vacuum cycle, the high and low temperature should be kept for 4 h for temperature stabilization (temperature fluctuation <0.5°C/h). The temperature change rate was about 3.7°C/min. The laboratory environment temperature was 18.9–24.2°C, and relative humidity (RH) was 33.7%–41.7%. After 6.5 cycles of thermal vacuum cycling test, the appearance of the SMPC-FSAS was checked, and all the components worked in normal. The resistance values before and after thermal vacuum cycling test were within the normal range. Note that, a deployment demonstration in the vacuum tank was also performed, which is discussed in the section of ground-based releasing and deployment evaluation.

3.2.3 Thermal cycling test in air

On the basis of thermal equilibrium test and thermal vacuum cycling test, in order to further ensure the reliability of SMPC-FSAS on orbit, a thermal cycling in air was performed (Figure 16). The temperature range was −117°C–+88°C. Temperature changing rate was 3.12°C/min. In each thermal cycling in air, the high and low temperature should be kept 4 h for temperature stabilization, with the temperature deviation 0°C–+4°C (high temperature) and −4°C–0°C (low temperature). The period of a single cycle was approximately 12 h, and the total duration was 227 h (9 d and 11 h) of 18.5 cycles. After all the tests, the heating tank was opened, the appearance and function of the SMPC-FSAS were checked. The resistance values before and after thermal cycling test were within the normal range (3 channels of heating, 6 channels of temperature measurement, and 1 channel of limit switch). After experiencing the thermal cycling test in air, the reliability of the SMPC-FSAS was verified.

Through the above thermal performance tests, the fol-

Table 6 Summary of the extreme temperatures in different thermal conditions

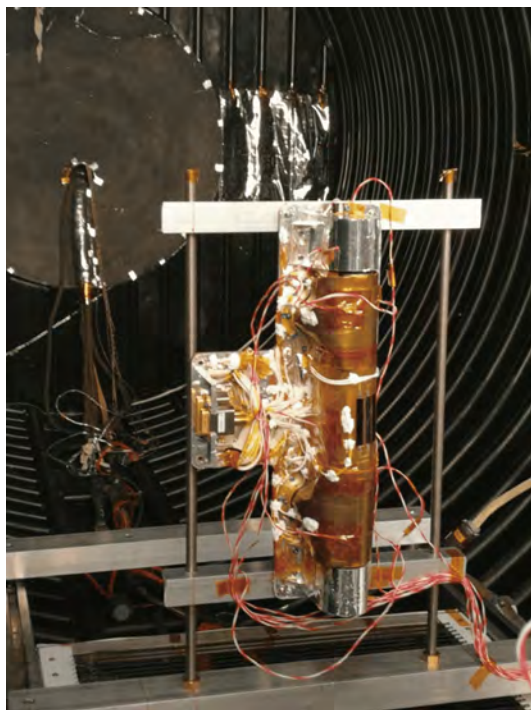| Temperature	Epoxy-based SMPC tubes	Cyanate-based SMPC locking laminate
Extremely-high temperature of steady-state thermal equilibrium (°C)	73.23	37.84
Extremely-high temperature of transient-state thermal equilibrium (°C)	72.06	34.81
Extremely-low temperature of transient-statethermal equilibrium (°C)	−101.90	−73.36

Figure 15 Setup of thermal vacuum cycling test of SMPC-FSAS flight hardware.

Figure 16 Thermal cycling test in air of the SMPC-FSAS flight hardware.

lowing reliabilities of the SMPC-FSAS in space environment were basically validated: the locking and releasing function of cyanate-based SMPC releasing mechanism, and the deployment function of epoxy-based SMPC tubes. Note that, for the SMPC-FSAS flight hardware in a deployed configuration, its structural stiffness is the most important which has been tested using sinusoidal sweeping vibration test as shown in Figure 11, and the thermal cycling tests were not performed due to the extremely high cost.

4 On-orbit demonstration of the SMPC-FSAS aboard SJ20 Geostationary Satellite

After completing the ground-based tests of the structures and functions, the SMPC-FSAS was mounted on the east deck of SJ20 Satellite as shown in Figure 17. Together with SJ20 Satellite, the following ground-based tests of SMPC-FSAS were further conducted, including structure and reliability tests (vibration, thermal test, electromagnetic compatibility, etc.), and functional tests (releasing and deployment on the SJ20 Satellite). In particular, the releasing mechanisms proposed in this paper have testability, which show advantages compared with traditional electro-explosive devices.

The SJ20 Geostationary Satellite, equipped with the SMPC-FSAS, was successfully launched aboard the Long-March-5 Y3 Heavy Rocket in Wenchang Satellite Launch Center on 27 Dec. 2019. The locking function of the SMPC releasing mechanisms of SMPC-FSAS was in normal during launch process. After multiple orbital transfers, the SJ20 Geostationary Satellite was positioned in a pre-determined geostationary orbit at a distance of about 36000 km from the surface of earth. On 5 Jan. 2020, selecting the position al-
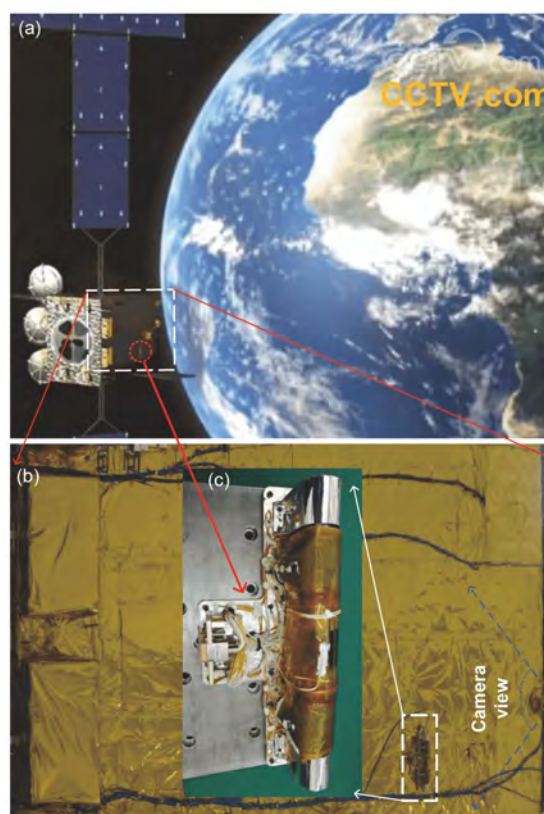

Figure 17 The stowed configuration of the SMPC-FSAS flight hardware mounted on the east deck of the SJ20 Geostationary Satellite. (a) Illustration of SJ20 Geostationary Satellite (screenshot from the video of [35]); (b) SMPC-FSAS flight hardware mounted on the east deck; (c) SMPC-FSAS flight hardware.

lowed for lighting and optical camera views, the on-orbit demonstration of SMPC-FSAS was carried on, and it successfully released and deployed as shown in Figure 18. Table 7 lists the primary results of on-orbit demonstration of SMPC-FSAS, including power-up and power-down times for unlocking of releasing mechanisms, deployment of flexible solar array system, and deployment of other SMP parts. For details, during the releasing process, the total heating period of releasing mechanism was 234 s, and the triggering signal of limit switches returned to ground was at the 139 s (Figure 18(a)). It indicated that the lateral displacement of pin pullers of two releasing mechanisms both approached 7 mm. It further revealed that the two releasing mechanisms had successfully unlocked, because the displacement of pin pullers for unlocking was just 4 mm.

To monitor the deployment process of SMPC flexible solar array system, the surveillance camera located on the edge of east deck was employed by using the fast transmission channels of the star-ground link with negligible time delay (5 frames per second, developed by Zhejiang University). Based on the images returning to the ground from the SJ20 Geostationary Satellite, the SMPC-FSAS achieved approximate 100% shape recovery ratio within 60 s as shown in Figure 18(b). Upon heating, in 0–10 s, the deployment movement of flexible solar array system was slow. In 10–30 s, the deployment movement was relatively fast. In 30–60 s, the flexible solar array system slowly approached an approximate 100% shape recovery ratio based on the indication of surveillance camera.

5   Discussion

SMPs and SMPCs were studied since 2006 in Jinsong Leng's group in Harbin Institute of Technology, China. Several types of SMPs were developed for applying in aerospace conditions including epoxy-based [36], cyanate-based [37] and polyimide-based [38] SMPs with the T_g in the range of 60°C–323°C. Moreover, in order to promote the realistic aerospace application of SMPCs, we have conducted three projects of on-orbit demonstrations in different levels, namely material-level (rollable SMPC laminate on SJ17 Geostationary Satellite in Nov. 2016 [33]), part-level (SMPC hinges and shape-memory-alloy releasing device on SJ18 Geostationary Satellite in July 2017 [34]), system-level (a
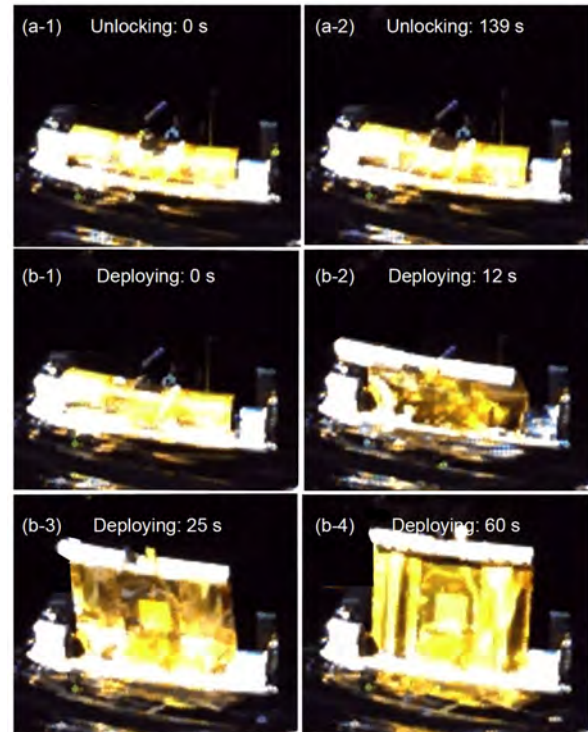

Figure 18   On-orbit releasing and deployment demonstration of the SMPC-FSAS flight hardware which was performed on SJ20 Geostationary Satellite on 5 Jan., 2020. (a-1), (a-2) Unlocking process in space; (b-1)–(b-4) deploying process in space.

flexible solar array system mainly fabricated by SMPCs on SJ20 Geostationary Satellite in Dec. 2019). The rolled epoxy-based SMPC laminate was on-orbit successfully deployed on SJ17 Geostationary Satellite in Nov. 2016. Moreover, a solid solar panel system, which was locked by one shape-memory-alloy releasing device and actuated by two pairs of epoxy-based SMPC hinges, was ground-based validated and launched aboard SJ18 Geostationary Satellite on 2 July 2017. In the first 900 s during launching, the locking function of the solid solar panel system was in normal. However, unfortunately, due to the failure of Long-March-5 Y2 Heavy Rocket, the SJ18 Geostationary Satellite crashed together with the solid solar panels system. In this project, the flexible solar array system, which was mainly fabricated by SMPCs, was developed. The epoxy-based SMPC was used for the rolling-out variable-stiffness beams as a structural frame as well as an actuator for the flexible blanket solar array. The cyanate-based SMPC was used for

Table 7   Primary results of on-orbit demonstration of the SMPC-FSAS flight hardware which was performed on SJ20 Geostationary Satellite on 5 Jan., 2020

	Start time (hh:mm:ss)	Ending time (hh:mm:ss)	Results
Unlocking of releasing mechanisms	03:16:06	03:20:00	Releasing in normal; unlocking signal returned to ground at 03:18:25
Deployment of flexible solar array system	03:22:20	03:25:20	Deployment in normal; recovering ratio 100%
Deployment of other SMP parts	03:31:28	03:32:28	Deployment in normal; recovering ratio 100%

releasing mechanism. The flexible solar array system was successfully validated on SJ20 Geostationary Satellite on-orbit on 5 Jan., 2020.

For a space deployable structure made of traditional materials, the unlocking or deployment process usually takes a very short period of time, and it may cause serious transient vibration and shocking of spacecraft. During this on-orbit experiment, the SMPC-FSAS successful realized the controllable releasing and deployment based on SMPC materials without traditional electro-explosive devices, hinges, motors/controllers or complex mechanical mechanisms. The releasing mechanism of SMPC-FSAS realized low impact, testability and high reliability as a new releasing mechanism, which showed the possibility to replace traditional electro-explosive device. The flexible solar array system of SMPC-FSAS has successful deployed on the basis of shape memory effect of SMPC. It also showed the possibility to overcome problems of high impact and unstable deployment of traditional deployment mechanisms, and to replace the traditional space rigid mechanical systems in some cases.

The SMPC smart structures in this paper have realized the integration of structures and functions, including the function of locking and releasing, controllable deployment, and deployed high structural stiffness. They showed the advantages of extremely-low impact during unlocking process, controllable deployment with extremely-low impact, and high rigidity after deployment. Based on the large deformation characteristics (as high as 10% compressive strain in macro scale) of SMPC materials, the limit area of deployed structures would be much larger than that made of conventional rigid thin-wall materials. The SMPC material can be applied for ultra-large space deployable structures with a relative high deployed stiffness and strength.

The world's first spaceflight on-orbit demonstration of the SMPC-FSAS may accelerate the related study and production to be applied for the next-generation releasing mechanisms and space deployable structures, such as new releasing mechanisms with low-shocking, testability and reusability, and ultra-large space deployable solar array.

Note that, the contents in the current paper are a general design and overall introduction for the SMPC-FSAS flight hardware. In near future, more papers will be released to further discuss the details of SMPC-FSAS, including cyanate-based SMPC releasing mechanism, structural design and analysis of SMPC-FSAS, thermal design and analysis of SMPC-FSAS.

6   Conclusions

The SMPC-FSAS consists of a pair of rolling-out epoxy-based SMPC variable-stiffness tubes with clamping one piece of flexible blanket solar array, and a pair of cyanate-based SMPC releasing mechanisms. To ensure the mechanical reliability, numerous ground-based tests of SMPC-FSAS were carried out, including structural dynamics performance, thermal performance, releasing and deployment evaluation. The locking function of the SMPC releasing mechanisms of the SMPC-FSAS flight hardware was in normal when launching aboard the SJ20 Geostationary Satellite on 27 Dec. 2019. On 5 Jan., 2020, the SMPC-FSAS successfully unlocked and deployed. The triggering signal of limit switches returned to ground at the 139 s, which revealed that the two releasing mechanisms successfully unlocked actuating by the cyanate-based SMPC laminates. The epoxy-based SMPC variable-stiffness tubes with lenticular cross section also deployed and slowly approached an approximate 100% shape recovery rate within 60 s upon heating.

As a completely new type of releasing mechanism, the SMPC releasing mechanisms of SMPC-FSAS realized low impact, repeatable testability, which shows the possibility to replace traditional electro-explosive devices in some low loading cases. Based on the large-deformation characteristics of SMPC with as high as 10% compressive strain in macro scale, the deployed limit area of SMPC structures may be much larger than those made of conventional thin-wall composites with 1.5%–2% reversible strain. Thus, the SMPC could be applied for ultra-large space deployable structures. The current study and on-orbit successful validation of the SMPC-FSAS may accelerate the related study and associated productions to be used for the next-generation releasing mechanisms as well as space deployable structures, such as new releasing mechanisms with repeatable testability, and ultra-large space deployable solar arrays.

1   Chilan C M, Herber D R, Nakka Y K, et al. Co-design of strain-actuated solar arrays for spacecraft precision pointing and jitter reduction. AIAA J, 2017, 55: 3180–3195

2   Okhotkin K G, Vlasov A Y, Zakharov Y V, et al. Analytical modeling of the flexible rim of space antenna reflectors. J Appl Mech Tech Phy, 2017, 58: 924–932

3   Lagrange R, López Jiménez F, Terwagne D, et al. From wrinkling to global buckling of a ring on a curved substrate. J Mech Phys Solids, 2016, 89: 77–95

4   Murphey T W, Francis W, Davis B, et al. High strain composites. In: 2nd AIAA Spacecraft Structures Conference. Kissimmee, Florida: AIAA, 2015. 0942

5   Lendlein A, Kelch S. Shape-memory polymers. Angew Chem Int Ed, 2002, 41: 2034

6   Leng J, Lan X, Liu Y, et al. Shape-memory polymers and their composites: Stimulus methods and applications. Prog Mater Sci, 2011, 56: 1077–1135

7   Leng J S, Du S Y. Shape Memory Polymer and Multifunctional Nanocomposite. London: CRC Press, 2010

8   Lan X, Liu Y, Lv H, et al. Fiber reinforced shape-memory polymer composite and its application in a deployable hinge. Smart Mater Struct, 2009, 18: 024002

9   Liu Y, Du H, Liu L, et al. Shape memory polymers and their composites in aerospace applications: A review. Smart Mater Struct, 2014, 23: 023001

10 Auffinger F, Fisher M, Maddux M. Shape memory polymer (SMP) actuation technology, In: 2010 Conference on Sensors and Smart Structures Technologies for Civil, Mechanical, and Aerospace Systems. San Diego, 2010. 1–8

11 Koerner, H, Strong R J, Smith M L, et al. Polymer design for high temperature shape memory: Low crosslink density polyimides. Polymer, 2013, 54: 391–402

12 https://dss-space.com/

13 Spence B, White S. Directionally controlled elastically deployable roll-out solar array. US Patent, 8,683,755, 2014-04-01

14 Hoang B, Spence B, White S, et al. Commercialization of deployable space systems roll-out solar array (ROSA) technology for space systems loral (SSL) solar arrays. In: 2016 IEEE Aerospace Conference. Montana, 2016. 1–12

15 Spence B R, White S, LaPointe M, et al. International space station (ISS) roll-out solar array (ROSA) spaceflight experiment mission and results. In: 2018 IEEE 7th World Conference on Photovoltaic Energy Conversion (WCPEC). Hawaii, 2018. 3522–3529

16 Fang H, Li S, Ji H, et al. Dynamics of a bistable miura-origami structure. Phys Rev E, 2017, 95: 052211

17 Ko K E, Kim J H. Thermally induced vibrations of spinning thin-walled composite beam. AIAA J, 2003, 41: 296–303

18 Blumenschein L H, Gan L T, Fan J A, et al. A tip-extending soft robot enables reconfigurable and deployable antennas. IEEE Robot Autom Lett, 2018, 3: 949–956

19 Hu Y, Chen W, Gao J, et al. A study of flattening process of deployable composite thin-walled lenticular tubes under compression and tension. Compos Struct, 2017, 168: 164–177

20 Barrett R, Francis W, Abrahamson, et al. Qualification of elastic memory composite hinges for spaceflight applications. In: 47th AIAA/ASME/ASCE/AHS/ASC Structures, Structural Dynamics, and Materials Conference. Newport: AIAA, 2006. 1–10

21 Maji A K, Lips J A, Azarbayejani M. Measurement and analytical modeling of the deployment rate of elastic memory composites. Exp Mech, 2012, 52: 717–727

22 Lan X, Liu L, Liu Y, et al. Post microbuckling mechanics of fibre-reinforced shape-memory polymers undergoing flexure deformation. Mech Mater, 2014, 72: 46–60

23 Lan X, Hao S, Liu L, et al. Macroscale bending large-deformation and

24 microbuckling behavior of a unidirectional fiber-reinforced soft composite. J Compos Mater, 2020, 54: 243–257

25 Keller P, Lake M, Francis W, et al. Development of a deployable boom for microsatellites using elastic memory composite material. In: 45th AIAA/ASME/ASCE/AHS/ASC Structures, Structural Dynamics & Materials Conference. Palm Springs, 2004. 1603

26 López Jiménez F, Pellegrino S. Folding of fiber composites with a hyperelastic matrix. Int J Solids Struct, 2012, 49: 395–407

27 Lin J K H, Knoll C F, Willey C E. Shape memory rigidizable inflatable (RI) structures for large space systems applications. In: 47th AIAA/ASME/ASCE/AHS/ASC Structures, Structural Dynamics, and Materials Conference. Newport: AIAAA, 2006. 1–10

28 Zhang J, Dui G, Liang X. Revisiting the micro-buckling of carbon fibers in elastic memory composite plates under pure bending. Int J Mech Sci, 2018, 136: 339–348

29 Liu Y, Guo Y, Zhao J, et al. Carbon fiber reinforced shape memory epoxy composites with superior mechanical performances. Compos Sci Tech, 2019, 177: 49–56

30 Peffer A, Denoyer K, Fosness E, et al. Development and transition of low-shock spacecraft release devices. In: IEEE Aerospace Conference Proceedings, Vol 4. Big Sky, 2000. 277–284

31 Nava N, Collado M, Cabás R. REACT: Resettable hold down and release actuator for space applications. J Materi Eng Perform, 2014, 23: 2704–2711

32 Wei H, Liu L, Zhang Z, et al. Design and analysis of smart release devices based on shape memory polymer composites. Compos Struct, 2015, 133: 642–651

33 Zhao H, Lan X, Liu L, et al. Design and analysis of shockless smart releasing device based on shape memory polymer composites. Compos Struct, 2019, 223: 110958

34 Li F, Liu L, Lan X, et al. Ground and geostationary orbital qualification of a sunlight-stimulated substrate based on shape memory polymer composite. Smart Mater Struct, 2019, 28: 075023

35 Liu Z, Li Q, Bian W, et al. Preliminary test and analysis of an ultralight lenticular tube based on shape memory polymer composites. Compos Struct, 2019, 223: 110936

36 https://v.gmw.cn/2020-01/06/content_33458442.htm

37 Leng J, Wu X, Liu Y. Effect of a linear monomer on the thermomechanical properties of epoxy shape-memory polymer. Smart Mater Struct, 2009, 18: 095031

38 Xie F, Huang L, Liu Y, et al. Synthesis and characterization of high temperature cyanate-based shape memory polymers with functional polybutadiene/acrylonitrile. Polymer, 2014, 55: 5873–5879

39 Xiao X, Qiu X, Kong D, et al. Optically transparent high temperature shape memory polymers. Soft Matter, 2016, 12: 2894–2900